



Hydrological modeling using the SWAT Model in urban and peri-urban environments: The case of Kifissos experimental sub-basin (Athens, Greece)

5 Evgenia Koltsida¹, Nikos Mamassis², Andreas Kallioras¹

¹Laboratory of Engineering Geology and Hydrogeology, School of Mining and Metallurgical Engineering, National Technical University of Athens, Heroon Polytechniou Str. 9, 15780 Zografou, Athens, Greece

²Laboratory of Hydrology and Water Resources Development, School of Civil Engineering, National Technical University of Athens, Heroon Polytechniou Str. 9, 157 80 Zographou, Greece

10 *Correspondence to:* Evgenia Koltsida (evita.koltsida@gmail.com)

Abstract. SWAT (Soil and Water Assessment Tool) is a continuous time, semi-distributed river basin model that has been widely used to evaluate the effects of alternative management decisions on water resources. This study, demonstrates the application of SWAT model for streamflow simulation in an experimental basin with daily and hourly rainfall observations to investigate the influence of rainfall resolution on model performance. The model was calibrated for 2018 and validated for 15 2019 using the SUFI-2 algorithm in the SWAT-CUP program. Daily surface runoff was estimated using the Curve Number method and hourly surface runoff was estimated using the Green and Ampt Mein Larson method. A sensitivity analysis conducted in this study showed that the parameters related to groundwater flow were more sensitive for daily time intervals and channel routing parameters were more influential for hourly time intervals. Model performance statistics and graphical techniques indicated that the daily model performed better than the sub-daily model. The Curve Number method produced 20 higher discharge peaks than the Green and Ampt Mein Larson method and estimated better the observed values. Overall, the general agreement between observations and simulations in both models suggests that the SWAT model appears to be a reliable tool to predict discharge over long periods of time.

1 Introduction

Water resource problems, including the effects of urban development, alternative management decisions and future climate 25 oscillation on streamflow and water quality, require a deep understanding and accurate modeling of earth surface processes at the catchment scale in order to be addressed (Gassman et al., 2014). Experimental catchments provide databases of long-term historical hydrological data which are useful in analyzing the mechanisms governing surface runoff as well as for developing and validating watershed, water quality and water resources management models (Goodrich et al., 2020). They are also able to monitor the major components of the surface hydrological cycle by using remote sensing and geophysical 30 measurements (Tauro et al., 2018). Furthermore, they can monitor groundwater and river water quality with the use of tracer



experiments which can estimate the residence and travel times of water in different components of the hydrological cycle (Hrachowitz et al., 2016; Stockinger et al., 2016).

Bogena et al. 2018 presented an extensive overview of hydrological observatories that are presently operated worldwide with various environmental conditions. The US Department of Agriculture-Agricultural Research Service's (ARS) Experimental Watershed Network has operated over 600 watersheds in its history and currently operates more than 120 experimental hydrological watersheds (Goodrich et al., 2020). The USDA-ARS watersheds provide deep knowledge of watershed processes and contribute in the development and validation of numerous watershed models. In addition, many of the watersheds have been used as validation sites for satellite sensors. The Hinkson Creek Watershed (HCW) is an urbanizing agricultural experimental watershed, located in central Missouri, USA. The HCW contributes to the understanding of precipitation/discharge relationship in multiple-land-use watersheds and investigates the impact of land use on the hydrology regime and nutrient yields (Hubbart et al., 2019; Kellner and Hubbart, 2017; Nichols et al., 2016; Zeiger and Hubbart, 2016). Other well-monitored experimental catchments are the Critical Zone Observatories (CZO) in the United States (White et al., 2015), the Terrestrial Environmental Observatories (TERENO) in Germany (Zacharias et al., 2011), the Heihe Watershed Allied Telemetry Experimental Research (HiWATER) in China (Li et al., 2013) and the European Network of Hydrological Observatories (ENOHA) which is a network of hydrological observatories within Europe (Bogena et al., 2018).

Hydrological and water quality models have been widely used to assess water resource problems and to investigate hydrological processes, land use and climate change impacts and best management practices (Daggupati et al., 2015). In recent decades, various models have been developed to operate in several temporal and spatial scales and with different levels of input data and model structure complexity (Arnold et al., 2015). The SWAT (Soil and Water Assessment Tool) program is a physically based, semi-distributed, continuous time river basin model (Arnold et al., 2012). The model is an open source code and has five main official versions, SWAT2000, SWAT2005, SWAT2009, SWAT2012, and SWAT+. It has been applied to catchments of various sizes and to several temporal scales (e.g., monthly, daily and sub-daily time step). SWAT has two methods for the estimation of surface runoff; the SCS Curve Number (CN) method (Soil Conservation Service, 1972) for daily rainfall and the Green and Ampt Mein Larson infiltration (GAML) method (Mein and Larson, 1973) for sub-daily rainfall. The CN method has been used more often than the GAML method, in SWAT model applications, mainly due to the absence of high temporal resolution data needed for the sub-daily module (Bauwe et al., 2016; Brighenti et al., 2019; Gassman et al., 2014). The few available studies suggest that the calibrated streamflow results are more accurate using the CN approach when compared to the GAML approach (Bauwe et al., 2016; Cheng et al., 2016; Ficklin and Zhang, 2013; Kannan et al., 2007). In particular, in the study where CN improved the results, Kannan et al. (2007) identified a suitable combination of evapotranspiration and runoff generation methods and reported that the CN method performed better than the GAML method. In contrast, three studies reported that the GAML method simulated better the peak flows during the flood season than the CN method (Li and DeLiberty, 2020; Maharjan et al., 2013; Yang et al., 2016). Some studies, have pointed out that both approaches have limitations and that the improvement depends on the part of the hydrograph that is analyzed (e.g., high, medium or low flows) and the time scale (e.g., daily, monthly or annually) (Han et al., 2012; King et al.,



65 1999). Furthermore, several sub-daily applications have been conducted such as land use and management impacts on flood
events (Golmohammadi et al., 2017; Campbell et al., 2018), the use of high temporal resolution data for the improvement of
the model (Bauwe et al., 2017; Boithias et al., 2017) and modeling of rainfall-runoff events (Jeong et al., 2010; Yu et al.,
2018). The authors generally found that finer temporal resolution time steps do not always improve model performance but
depend on the basin scale and the characteristics of the watershed. A detailed description of the model history and
70 applications can be obtained in Gassman et al. (2007), Douglas-Mankin et al. (2010), Brighenti et al. (2019) and Tan et al.
(2020).

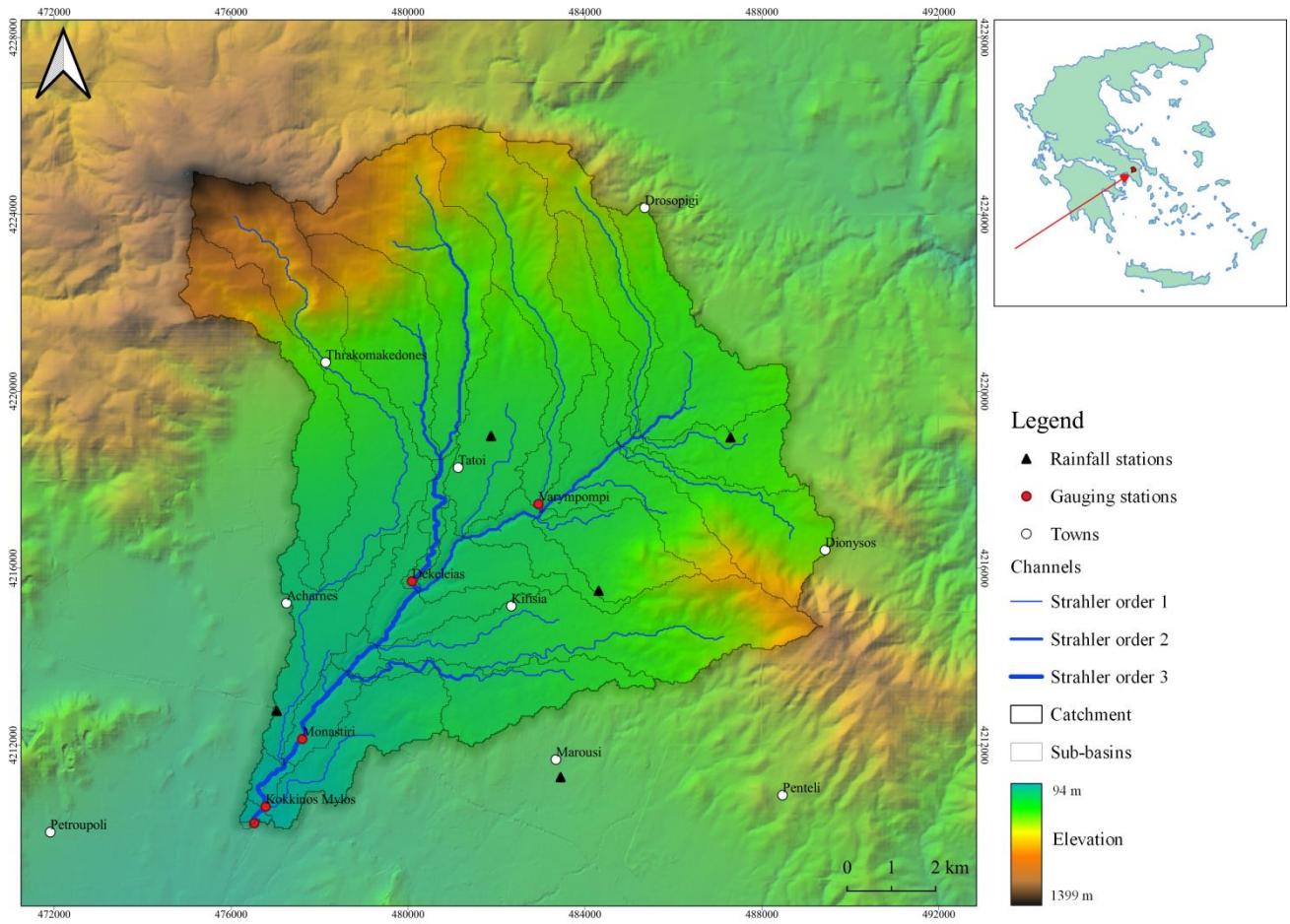
In this study, the latest version of SWAT was used to simulate streamflow in an experimental basin using daily and sub-
daily (hourly) rainfall observations in order to estimate the influence of rainfall resolution on model performance. To
calibrate the model, water level data were obtained from the river gauge located at the basin outlet. The model calibration
75 and uncertainty assessment were achieved using the Sequential Uncertainty Fitting program (SUFI-2) in SWAT-CUP
software (Abbaspour et al., 2004, 2007). The information of the study area, methodology and data input is presented in
Section 2, results and discussions are detailed in Section 3 and conclusion is provided in Section 4.

2 Materials and methods

2.1 Study area

80 The study area includes the upper part (NW sub-basin) of the Kifissos River basin, located in Athens Greece (Fig. 1). The
Kifissos River basin occupies an area of 380 km² and its route is approximately 22 km, of which at least 14 km are within an
urban area. The elevation ranges from 94 m to 1399 m with plains in the south and hills in the north part of the basin. The
mean annual temperature is 16.4 °C and the mean annual rainfall across the basin is 577.2 mm.

The study area is characterized as an urban/sub-urban area, with residential areas, shrubland and agriculture accounting for
85 34.1, 15.9 and 12.4 % of its land use coverage, respectively (Fig. 2a). It includes mainly four soil types, Cambisols,
Regosols, Leptosols and Luvisols (Fig. 2b). The dominant soil formations are characterized by good soil permeability and
high contents of clay and sand.



90 **Figure 1. Geographical location of the study area.**



(a) Land Use

(b) Soil

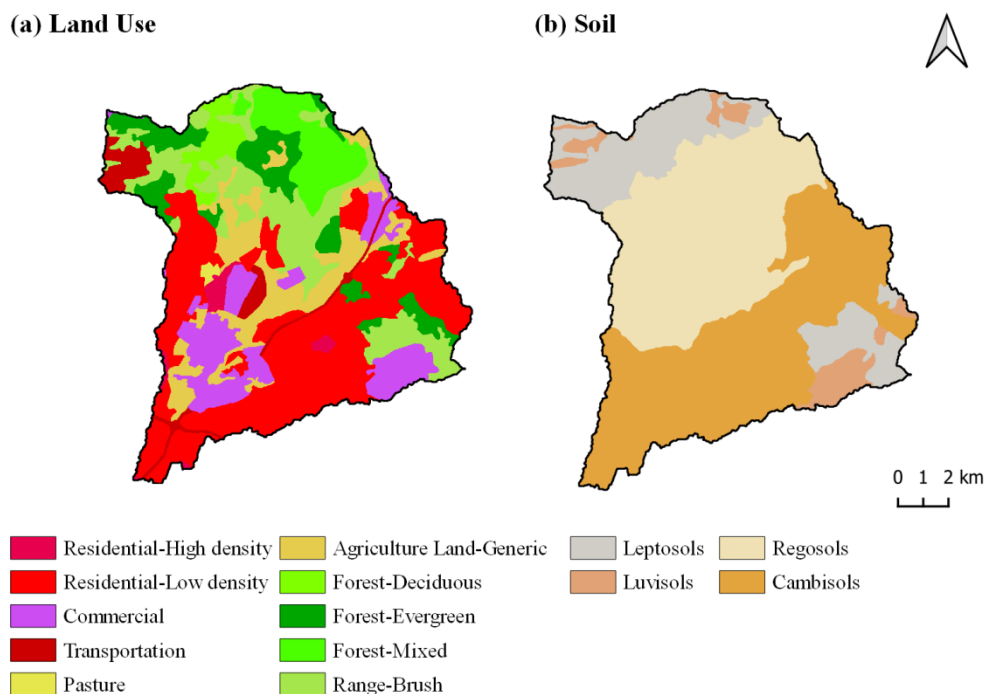


Figure 2. Spatial distribution of land use and soil.

2.2 Experimental Catchment of Athens Metropolitan Area

95 The study area includes four in-site monitoring stations measuring water level and water velocity on the river in different times and under different weather conditions (Fig. 1). The stations were installed at the end of 2017 under the supervision of the School of Mining of NTUA. The network was developed under the European SCENT (Smart Toolbox for Engaging Citizens in a People-Centric Observation Web) program. The station which is located at the outlet of the study area was selected as the most suitable for further analysis in this study, because the three upstream stations were out of order for a long time and continuous discharge time series were not available for calibration and validation.

100 The pressure measurement sensor was an Adcon LEV1 Level Sensor (pressure transducer), with 0.1% distance measurement accuracy from the target. The automatic level measurement sensor was a Pulsar dBi intelligent transducer (ultrasonic measurement transducer) with reliable measurement from 125 mm to 15 m. The Stylitis-20 data logger was connected to the sensor. The data logger also offers the possibility to either download the data in situ or remotely transfer data through the use of the built in GSM/GPRS modem. The time step for transmitting the water level information has been set to 15 minutes.

105 The water level and water velocity data are provided freely from Open Hydrosystem Information Network (OpenHi.net).



2.3 Data sources

The input data for the construction of the SWAT model include a digital elevation model (DEM), a land use map, a soil map, and meteorological data (i.e., rainfall, temperature, wind speed, relative humidity and solar radiation). Table 1 summarizes the input data along with their sources, used in this study.

The digital elevation model (DEM) at 30 m spatial resolution was downloaded from the website of the US Geological Survey (USGS). The land use map was derived from the 100 m 2018 Corine Land Cover map (CLC, 2018) and was modified according to SWAT land use categories (Table 2). The soil map was created from data of the Food and Agriculture Organization (FAO) Digital Soil Map of the World (FAO et al., 2012). In addition, rainfall data, relative humidity, wind speed, and the minimum and maximum air temperature were obtained from National Observatory of Athens (NOA). Solar radiation data were simulated by WGEN, a weather generator developed by SWAT to fill the missing meteorological data by the use of monthly statistics. A rain gauge network consisting of 5 gauges is distributed throughout the study area as illustrated in Fig. 1. Daily and hourly ($\Delta t = 1\text{h}$) rainfall data were retrieved from 2017 to 2019 with coverage during the entire year. The daily and sub-daily observed streamflow data at the outlet of the basin (Fig. 1) from 2017 to 2019 were acquired from Open Hydrosystem Information Network (OpenHi.net).

Table 1. SWAT model input data and sources.

Data type	Resolution	Source	Description
DEM	30 m × 30 m	Shuttle Radar Topography Mission https://earthexplorer.usgs.gov/	Digital elevation model
Land use	100 m × 100 m	Corine Land Cover https://land.copernicus.eu/	Land use map
Soil	30 arcseconds (1:5.000.000)	Food and Agriculture Organization, http://www.fao.org/	Soil map
Weather data	5 gauges	National Observatory of Athens, https://www.meteo.gr/	Daily data for 2017-2019, sub-daily data for 2017-2019, minimum and maximum air temperatures, relative humidity, wind speed
Observed streamflow	1 gauge	Open Hydrosystem Information Network, https://openhi.net/	Daily data for 2017-2019, sub-daily data for 2017-2019



Table 2. Land use classification of the Kifissos basin and the corresponding SWAT land use category.

CLC code	Corine description	SWAT code	SWAT description	(%) Watershed
121	Industrial or commercial units	UCOM	Commercial	11.43
112	Discontinuous urban fabric	URLD	Residential-Low Density	34.11
122	Road and rail networks and associated land	UTRN	Transportation	4.07
111	Continuous urban fabric	URHD	Residential-High Density	1.54
231	Pastures	PAST	Pasture	0.31
243	Land principally occupied by agriculture, with significant areas of natural vegetation	AGRL	Agricultural Land-Generic	12.39
311	Broad-leaved forest	FRSD	Forest-Deciduous	3.11
312	Coniferous forest	FRSE	Forest-Evergreen	9.59
313	Mixed forest	FRST	Forest-Mixed	7.51
323	Sclerophyllous vegetation	RNGB	Range-Brush	15.94

130

2.4 Soil Water Assessment Tool (SWAT)

The SWAT (Soil and Water Assessment Tool) program is a semi-distributed, continuous-time, process based model (Arnold et al., 1998, 2012). The model operates on a daily time step and has been developed to evaluate the impact of management practices on water, sediment and agricultural chemical yields in large river basins over long time periods. The main components of SWAT are hydrology, weather, soil properties, land use, crop growth, sediments, nutrients, pesticides, bacteria and pathogens.

In SWAT, a watershed is divided into multiple sub-basins, which are then subdivided into hydrologic response units (HRUs) based on unique soil, slope and land use attributes. Hydrologic response units (HRUs) enable the model to represent differences in evapotranspiration for various types of vegetation and soil. Simulation of the hydrology of a watershed can be separated in the land phase, which determines the loadings of water, sediment, nutrients, and pesticides to the main channel, and in the routing phase, which is the movement of the loadings through the streams of the subbasins to the outlets (Neitsch et al., 2011).

Hydrological processes are simulated separately for each HRU, including canopy storage, surface runoff, partitioning of the precipitation, infiltration, redistribution of water within the soil profile, evapotranspiration, lateral subsurface flow from the soil profile, and return flow from shallow aquifers (Gassman et al., 2007). SWAT uses a single plant growth model to simulate all types of vegetation and is capable to differentiate between annual and perennial plants. The plant growth model estimates the amount of water and nutrients removed from the root zone, transpiration and biomass/yield production.

The main difference between the daily and sub-daily simulation in SWAT occurs in the estimation of surface runoff. The SCS Curve Number (CN) method (Soil Conservation Service, 1972) is used for daily simulations and the Green and Ampt



150 Mein Larson infiltration (GAML) method (Mein and Larson, 1973) is used for sub-daily simulations. The CN method is an empirical model, widely used, and requires land use, soil, elevation and daily rainfall data as input. The GAML method is a physically based model, uses the same spatial coverages as the CN method, and requires more detailed soil information and sub-daily rainfall records as input. More details on model theory, equations and processes can be found in Arnold et al. (1998), in Gassman et al. (2007) and in Neitsch et al. (2011).

155 **2.5 Model setup**

The latest version of the SWAT 2012 hydrological model was used in this study. The QSWAT plugin (Dile et al., 2016) embedded in QGIS platform was used for the setup and the parameterization of the model. The watershed delineation, stream parameterization and overlay of soil, land use and slope were automatically completed within the interface. A drainage area of 3.6 km² was chosen to discretize the study area. The area was delineated into 25 sub-basins, which were
160 then divided into 175 hydrological response unit (HRUs).

The SWAT models for the Kifissos basin include daily and sub-daily (hourly) rainfall observations. Potential evapotranspiration was calculated by the Penman-Monteith method, surface runoff was estimated using the CN method for the daily model and the GAML method for the hourly model, and the variable storage coefficient method was used to calculate the channel routing. The simulation period was from 2017 to 2019 and the first year was used as a warm-up period
165 in order to mitigate the unknown initial conditions. The model was calibrated from 01/01/2018 to 31/12/2018 and validated from 01/01/2019 to 31/12/2019 for discharge, using the SUFI-2 program in SWAT-CUP software (Abbaspour et al., 2004, 2007).

2.6 Sensitivity Analysis, Model Calibration and Validation

Watershed models are characterized by large uncertainties related to conceptual design, input data and parameters
170 (Abbaspour et al., 2015).

The model calibration, validation, and uncertainty analysis were achieved with the use of the SUFI-2 algorithm in the SWAT-CUP software (Abbaspour et al., 2004, 2007). In SUFI-2, uncertainties in parameters (e.g., uncertainty in input data, conceptual model, parameters and measured data) are expressed as ranges or uniform distributions. The concept behind this algorithm is to collect most of the observed data within a narrow uncertainty band. The initial ranges of the calibrating
175 parameters are set, based on literature and sensitivity analyses. Then, parameter sets are generated using Latin hypercube sampling and the objective function is estimated for each parameter set. The uncertainties are calculated at the 2.5% and 97.5% levels of the cumulative distribution of all output variables, and it is referred to as the 95% prediction uncertainty (95PPU). The goodness of model performance and output uncertainty are assessed using the P-factor and the R-factor (Abbaspour et al., 2004). The P-factor is the percentage of measured data bracketed by the 95PPU band and it ranges from 0
180 to 1, where 1 means all of the measured data are within model prediction uncertainty. The R-factor is the ratio of the average width of the 95PPU band and the standard deviation of the measured data. The values of R-factor range from 0 to infinity,



where a value near 0 reflects an ideal situation. The spatial scale of the project and the accuracy of the observed data affect the values of the P-factor and the R-factor (Abbaspour et al., 2015). In this study the Nash-Sutcliffe model efficiency (NS) was used as an objective function for both daily and sub-daily calibration and validation. The sensitivities of the parameters were estimated using the following equation (Eq. 1) (Abbaspour et al., 2015):

$$g = a + \sum_{i=1}^m \beta_i b_i, \quad (1)$$

where g is the goal function and b_i 's are the parameters selected for calibration. The sensitivities are calculated as average changes in the objective function which result from changes in each parameter, while all other parameters are changing. A t-test is then conducted to evaluate the significance of each parameter b_i . Parameters with large t-stat and small P-value were characterized as sensitive parameters.

Model validation was achieved using the calibrated parameter ranges without any further changes and the model performance of the calibration period was compared to the model performance of the validation period. The year 2017 was set as a warm-up period, the streamflow data from the year 2018 were used for calibration and the streamflow data from the year 2019 were used for validation. The statistics on annual precipitation and daily discharge were calculated for each period to overcome biases in discharge patterns. Annual precipitation for 2018 was 566 mm and annual precipitation for 2019 was 735 mm. Mean and standard deviation for 2018 were 1.25 and 0.46 and for 2019 were 1.42 and 0.74 respectively. These statistics ensure that the selected periods represent both wet and dry conditions. In the calibration and validation process, 18 parameters (Table 3) were used. About 600 simulations per iteration were conducted, and up to three iterations, until the results of P-factor and R-factor were satisfying.

Further evaluation of the model performance was achieved with the use of graphical and statistical techniques (Daggupati et al., 2015b; Harmel et al., 2014; Moriasi et al., 2007, 2015). Most commonly used statistical techniques are Nash-Sutcliffe efficiency (NSE) (Nash and Sutcliffe, 1970) coefficient of determination (R^2) (Moriasi et al., 2007) and percent bias (PBIAS) (Gupta et al., 1999) as shown in Eqs. (2), (3), and (4). Most commonly graphical techniques are time series charts, scatter plots, bar charts, maps and percent exceedance probability curves. The statistics were calculated for both models and then their performance was discussed according to guidelines given by (Moriasi et al., 2007, 2015).

$$R^2 = \frac{[\sum_{i=1}^n (Q_{obs}(i) - \bar{Q}_{obs})(Q_{sim}(i) - \bar{Q}_{sim})]^2}{\sum_{i=1}^n (Q_{obs}(i) - \bar{Q}_{obs})^2 \sum_{i=1}^n (Q_{sim}(i) - \bar{Q}_{sim})^2}, \quad (2)$$

$$NS = 1 - \left[\frac{\sum_{i=1}^n (Q_{obs}(i) - Q_{sim}(i))^2}{\sum_{i=1}^n (Q_{obs}(i) - \bar{Q}_{obs})^2} \right], \quad (3)$$

$$PBIAS = \left[\frac{\sum_{i=1}^n (Q_{obs}(i) - Q_{sim}(i)) * 100}{\sum_{i=1}^n Q_{obs}(i)} \right], \quad (4)$$



where Q_{obs} is the observed discharge, Q_{sim} is the simulated discharge on day i , \overline{Q}_{obs} is the mean of observed discharge and \overline{Q}_{sim} is the mean of simulated discharge. R^2 is a measure of how well the variance of measured data is replicated by the
215 model. R^2 can range from 0 to 1, where 0 means no correlation and 1 indicates perfect correlation and less error variance. NSE is a measure of how well the simulated values match the observed values. NSE can range from $-\infty$ to 1, where values \leq 0 show that the observed data mean is a more accurate predictor than the simulated values and 1 is a perfect fit between simulated and observed values. PBIAS, measures the average tendency of the simulated values to be larger or smaller than the observed values. The optimum value is 0, positive values show model underestimation and negative values show model
220 overestimation. More information about the strengths, weaknesses, and usage of the commonly used measures is presented in Moriasi et al. (2015). The SWAT-CUP software is designed mainly for daily, monthly or annually time step. In order to calibrate the sub-daily model, the SUFI-2 files required minor modifications.

**Table 3. Daily and sub-daily SWAT calibrated parameters. The method “r” indicates that the parameter value is multiplied by (1 + a given value), the method “v” indicates that the parameter value is going to be replaced and the method “a” indicates that the
225 parameter is to be added by a given value (Abbaspour et al., 2007).**



	Parameter	File Ext	Method	Description
Surface runoff	CN2	.mgt	r Relative	Curve number
	SURLAG	.bsn	v Replace	Surface runoff lag time
Groundwater/Baseflow	ALPHA_BF	.gw	v Replace	Baseflow alpha factor
	GW_DELAY	.gw	a Absolute	Groundwater delay
	RCHRG_DP	.gw	v Replace	Deep aquifer percolation fraction
	REVAPMN	.gw	v Replace	Threshold depth of water in the shallow aquifer for “revap” to occur
	GW_REVAP	.gw	v Replace	Groundwater “revap” coefficient
	GWQMN	.gw	v Replace	Threshold depth of water in the shallow aquifer required for return flow to occur
Lateral flow	LAT_TTIME	.hru	v Replace	Lateral flow travel time
	HRU_SLP	.hru	r Relative	Average slope steepness
Channel	OV_N	.hru	r Relative	Manning's "n" value for overland flow
	SLSUBBSN	.hru	r Relative	Average slope length
	CH_N2	.rte	v Replace	Manning's “n” value for the main channel
	CH_K2	.rte	v Replace	Effective hydraulic conductivity in main channel alluvium
Soil	ESCO	.bsn	v Replace	Soil evaporation compensation factor
	SOL_K	.sol	r Relative	Saturated hydraulic conductivity of the soil layer
	SOL_BD	.sol	r Relative	Moist bulk density
	SOL_AWC	.sol	r Relative	Available water capacity of the soil layer

3 Results and Discussion

230 3.1 Parameter’s sensitivity analysis and calibration

The most sensitive parameters obtained in daily and hourly simulation are presented in Table 4. Sensitive parameters are characterized by large t-Test and small p-Value. The parameters were characterized as significantly sensitive when the p-value was less than 0.03.

In the daily model, the most sensitive parameters were deep aquifer percolation fraction (RCHRG_DP), groundwater delay
 235 time (GW_DELAY), lateral flow travel time (LAT_TTIME), average slope steepness (HRU_SLP) and moist bulk density (SOL_BD). These parameters were connected to groundwater flow, runoff generation and channel routing. In the sub-daily model, the significantly sensitive parameters were average slope steepness (HRU_SLP), Manning’s “n” value for the main channel (CH_N2), effective hydraulic conductivity in main channel alluvium (CH_K2) and lateral flow travel time (LAT_TTIME). These were all related to channel routing.



240 The choice of model operational time step has an impact on the sensitivity of the SWAT parameters (Jeong et al., 2010). The
 parameters related to groundwater flow and runoff generation (GW_DELAY, RCHRG_DP) were more sensitive for the
 daily time intervals and the parameters regarding channel routing (HRU_SLP, LAT_TTIME, CH_N2, CH_K2) were more
 sensitive for the hourly time intervals. According to Boithias et al. (2017), the CH_N2 parameter is more sensitive at the
 hourly time step rather than the daily time step, because at the daily time step the flow peak is influenced by other processes
 245 decreasing the sensitivity of the CH_N2. Overall, in both daily and sub-daily models, channel routing was a very important
 factor for the simulation of the SWAT models.

The sub-daily model is characterized by larger GWQMN and GW_REVAP values than the daily model. GWQMN is the
 threshold depth of water in the shallow aquifer required for return flow to occur and GW_REVAP controls the water
 movement from the shallow aquifer into the overlying unsaturated soil layers. As these parameters increase, the rate of
 250 evaporation increases up to the rate of potential evapotranspiration, resulting in a corresponding decrease of the baseflow.
 The fitted value of CH_N2 in hourly simulation was $0.11(m^{-1/3}s)$ and was larger than $0.08(m^{-1/3}s)$ in the daily simulation.
 The CH_N2 parameter affects the rate and the velocity of flow (Boithias et al., 2017). Therefore, the larger CH_N2 value
 was connected to smaller flow velocity. In addition, the value range for CN2 was smaller for the sub-daily model, leading
 thereby to lower peak flows. Other differences were average slope steepness (HRU_SLP), average slope length
 255 (SLSUBBSN), groundwater delay time (GW_DELAY) and Manning's "n" value for overland flow (OV_N). Their values
 were all smaller in sub-daily simulation. The differences between the two models lay mostly in the different runoff
 estimation methods used by the two models.

It is worth noting that the observations, procedures and assumptions made for this study may affect the results of this study.
 The values of the calibrated parameters and their sensitivities are influenced by the type and quality of input data, the
 260 conceptual model, the choice of the objective function and inaccuracies in measured input data used for calibration and
 validation (Abbaspour et al., 2015; Arnold et al., 2012; Polanco et al., 2017).

Table 4. Daily and sub-daily SWAT calibrated parameters and their sensitivities.

Parameters	Initial ranges		Daily model				Sub-Daily model			
	Min	Max	t-Test	p-Value	Calibrated ranges		t-Test	p-Value	Calibrated ranges	
					Min	Max			Min	Max
CN2	-0.10	0.10	0.38	0.70	-0.04	0.10	-0.09	0.93	0.00	0.10
SURLAG	0.00	10.00	0.40	0.69	0.00	10.00	-0.36	0.72	4.00	9.00
ALPHA_BF	0.00	1.00	-0.15	0.88	0.05	0.69	-0.23	0.82	0.50	1.00
GW_DELAY	-30.00	90.00	4.78	0.00	10.00	95.00	0.51	0.61	10.00	80.00
RCHRG_DP	0.00	0.50	3.44	0.00	0.00	0.50	0.14	0.89	0.11	0.40
REVAPMN	1000.00	2000.00	1.51	0.13	990.00	1800.00	0.49	0.62	800.00	1800.00
GW_REVAP	0.02	0.20	-1.37	0.17	0.02	0.20	-0.16	0.87	0.06	0.21
GWQMN	0.00	500.00	0.69	0.49	100.00	500.00	0.38	0.71	150.00	500.00



LAT_TTIME	0.00	180.00	15.23	0.00	0.00	170.00	14.59	0.00	0.00	170.00
HRU_SLP	-0.50	3.00	-3.87	0.00	-0.01	3.00	-3.71	0.00	0.20	2.30
OV_N	-0.50	3.00	-0.94	0.35	-0.30	3.00	-0.73	0.47	-0.05	2.00
SLSUBBSN	-0.20	0.20	2.11	0.04	-0.10	0.20	0.89	0.37	-0.06	0.20
CH_N2	0.01	0.30	0.09	0.93	0.01	0.20	6.52	0.00	0.03	0.20
CH_K2	0.00	127.00	-0.83	0.41	0.00	80.00	3.52	0.00	0.00	50.00
ESCO	0.50	0.95	-0.43	0.67	0.50	0.95	-1.35	0.18	0.50	0.95
SOL_K	-0.80	0.80	-0.94	0.35	-0.20	0.80	-1.98	0.05	-0.10	0.68
SOL_BD	-0.30	0.30	-5.69	0.00	-0.10	0.30	-1.31	0.19	-0.01	0.27
SOL_AWC	-0.05	0.05	-1.53	0.13	-0.03	0.03	-0.90	0.37	-0.03	0.02

265 3.2 Daily and sub-daily model performances

Quantitative statistics and criteria recommended by Moriasi et al. (2007, 2015) were used to evaluate the model performance. Figure 3 shows the temporal dynamics of the hydrographs reproduced by both infiltration methods. The high flow season is observed during winter and spring. The low flow season is observed in summer and early fall due to high evapotranspiration. Figure 4 presents the flow duration curves of the two models, indicating good agreement between observed and simulated values. Generally, in the sub-daily model, the simulated discharge peaks did not always match the observed values and were sometimes considerably lower.

The performance statistics are illustrated in Table 5 and indicate reasonable calibrated models for both infiltration approaches. Model performance using the CN method showed better results than the GAML method. In particular, the NSE and R^2 indices for the daily model were 0.84 and 0.79 for the calibration period and 0.87 and 0.86 for the validation period. For the sub-daily model the NSE and R^2 indices were 0.53 and 0.49 for the calibration period and 0.63 and 0.6 for the validation period respectively. Furthermore, the daily model showed smaller modeling uncertainties with P-factor 0.79 and R-factor 1.58 (compared to 0.83 and 1.71 respectively for the sub-daily model).

Overall, the general agreement between the observed and the simulated values during the calibration and the validation period indicate that the choice of the calibration and validation periods was relevant. According to Moriasi et al. (2015) model performance can be evaluated as “satisfactory” for flow simulations if daily, monthly, or annual $R^2 > 0.60$, $NSE > 0.50$, and $PBIAS \leq \pm 15\%$ for watershed-scale models. These ratings should be modified to be more or less strict based on evaluation time step. Typically, model simulations are poorer for shorter time steps than for longer time steps (e.g., daily versus monthly or yearly) (Engel et al., 2007). Considering these guidelines, the daily and sub-daily models showed satisfactory performance for both calibration and validation periods.

The better performance of the CN method in comparison to the GAML method in this study is consistent with the results of other studies (Bauwe et al., 2016; Ficklin and Zhang, 2013; Kannan et al., 2007; King et al., 1999). Bauwe et al. (2016) evaluated both CN and GAML methods and highlighted that the CN method performed slightly better than the GAML



method. Ficklin and Zhang (2013) generally suggested that for daily simulations the CN method predicted more accurately streamflow as compared to the GAML model. Kannan et al. (2007) identified a suitable combination of ET runoff generation methods and reported that the CN method performed better than the GAML method. Kannan et al. (2007) conducted a sensitivity analysis to identify the best combination of evapotranspiration and runoff method for hydrological modeling and concluded that the CN method performed better than the GAML method for streamflow because the GAML method tends to hold more water in the soil profile and predict a lower peak runoff rate. King et al. (1999) concluded that the GAML method appeared to have more limitations in accounting for seasonal variability than the CN method.

290
295 In this study, the CN method produced higher discharge peaks than the GAML method and generally estimated better the observed values. The cause of these results could be that the choice of the sub-daily precipitation time step might be too large for this case. The selection of sub-daily precipitation input time step has a great impact on model results when using the GAML method and it should be based on the scale and characteristics of the watershed (Bauwe et al., 2016; Jeong et al., 2010; Kannan et al., 2007).

300

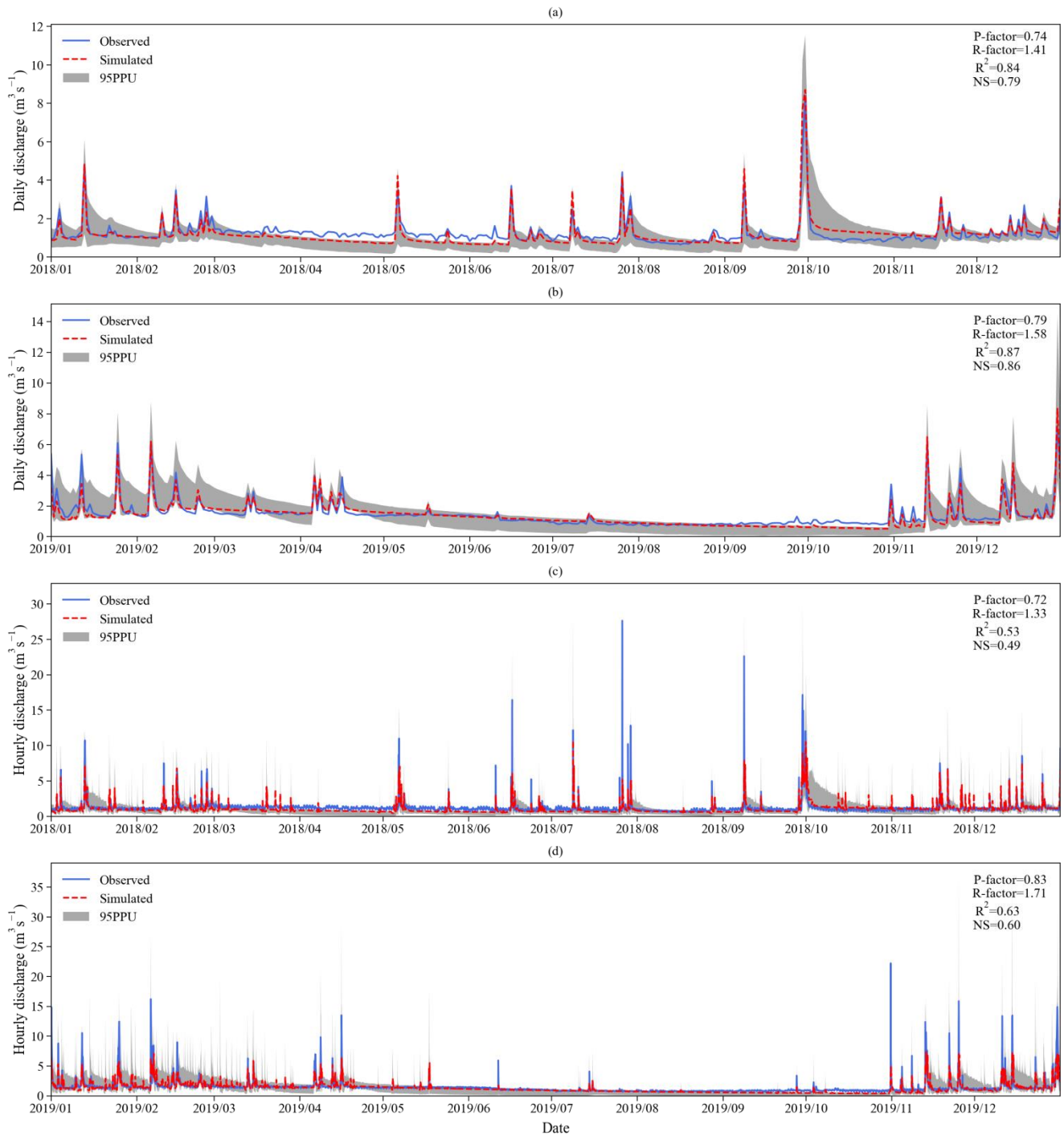


Figure 3. Observed and simulated discharge ($\text{m}^3 \text{s}^{-1}$) at the daily time step (a, b) and at the hourly time step (c, d).

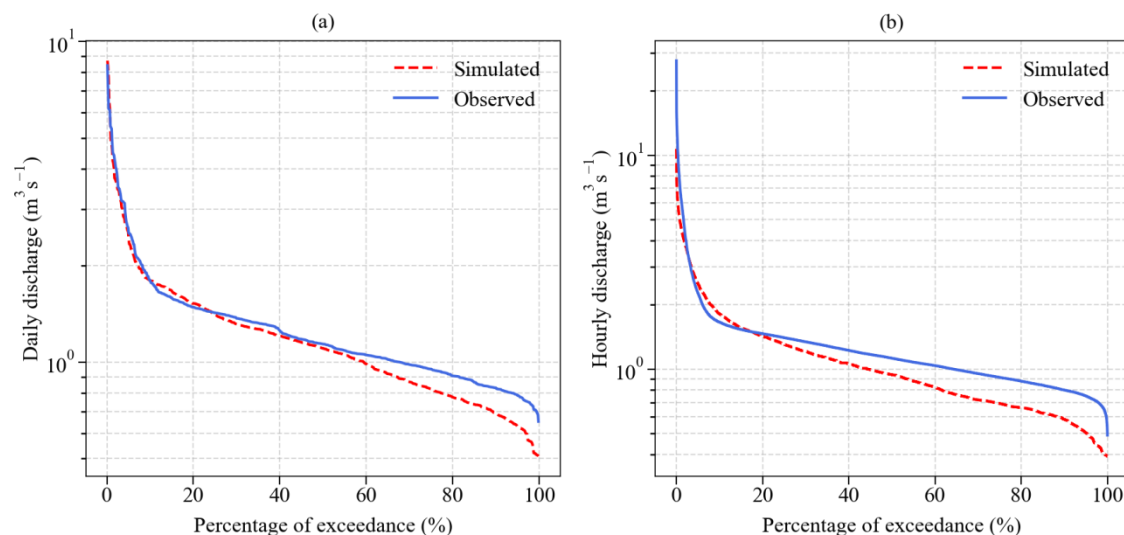


Figure 4. Observed and simulated flow duration curves ($\text{m}^3 \text{s}^{-1}$) at the daily time step (a) and at the hourly time step (b).

305

Table 5. Model evaluation statistics of the daily and sub-daily SWAT models for the calibration and validation periods.

Time-step	Period	p-Factor	r-Factor	R^2	NS	PBIAS(%)
Daily	Calibration	0.74	1.41	0.84	0.79	6.4
	Validation	0.79	1.58	0.87	0.86	4.2
Sub-Daily	Calibration	0.72	1.33	0.53	0.49	16.9
	Validation	0.83	1.71	0.63	0.6	11.7

3.3 Selected heavy rainfall events

Heavy rainfall events that occurred in the years 2018 and 2019 (Tatoi station, NOA records) were investigated in order to examine the accuracy of the sub-daily model and the impact of rainfall on an urban watershed. The hydrographs of the selected heavy rainfall events are presented in Figure 5.

The first event (Fig. 5a) is the precipitation of 32 mm during January 12 through January 14, 2018. On January 13th, the observed peak flow reached $10.6 \text{ m}^3/\text{s}$ at 4 am, $10.1 \text{ m}^3/\text{s}$ at 5 am and $10.7 \text{ m}^3/\text{s}$ at 6 am and the simulated peak flow were 5.8 , 7.1 and $5.7 \text{ m}^3/\text{s}$ respectively. The average observed discharge rate was $2.6 \text{ m}^3/\text{s}$ and the average simulated discharge rate was $2.2 \text{ m}^3/\text{s}$. The second event (Fig. 5b) is the precipitation of 27 mm during May 5 through May 7, 2018. The average observed discharge rate was $2.2 \text{ m}^3/\text{s}$ and the average simulated discharge rate was $2.1 \text{ m}^3/\text{s}$. On May 6th, the observed peak flow was $8.3 \text{ m}^3/\text{s}$ at 19 pm, $11 \text{ m}^3/\text{s}$ at 20 pm and $8.8 \text{ m}^3/\text{s}$ at 21 pm and the simulated peak flow were $6.1 \text{ m}^3/\text{s}$, $4 \text{ m}^3/\text{s}$ and $6.5 \text{ m}^3/\text{s}$ at the same time. The third event (Fig. 5c) is the precipitation of 56 mm during September 29 through October 1,



2018. About 31.4 mm were recorded from September 29th-10 am to September 30th-0 am. The average observed discharge
320 rate was 5.7 m³/s and the average simulated discharge was 5.2 m³/s. On September 29th, the observed peak flow reached 14.5
m³/s at 16 pm, 15.8 m³/s at 17 pm and continued to 17.2 m³/s at 18 pm. The simulated peak flows were 7.2, 6.1 and 8.9 m³/s
respectively. On September 30th, the peak flow reached to 10.1, 11.2, 12.1 m³/s at 18, 19 and 20 pm and model simulated
peak flow were 5.5, 7.8 and 9.5 m³/s.

The forth event (Fig. 5d) is the precipitation of 47.6 mm during February 5 through February 7, 2019. The simulated and
325 observed discharge reached to peak simultaneously but with different magnitude values. Specifically, on February 6th, the
peak flow reached to 7.5, 16.2 and 13.8 m³/s at 0, 1 and 2 am and model simulated peak flow were 6.2, 4.2 and 5.8 m³/s. The
average observed discharge rate was 3.6 m³/s and the average simulated discharge was 2.9 m³/s. The fifth event (Fig. 5e) is
the precipitation of 46.6 mm during November 12 through November 14, 2019. On November 13th, peakflow reached a peak
of 12.3 m³/s at 3 am but the model underestimated peak flow reaching only 3.5 m³/s. On the same day, the peak flow reached
330 to 9.3, 10.6 and 9.9 m³/s at 9, 10 and 11 am and the model simulated peak flow were 6.2, 7.4 and 6.7 m³/s. The average
observed discharge rate was 2.9 m³/s and the simulated discharge rate was 2.4 m³/s. The sixth event (Fig. 5f) is the intensive
precipitation of 99.6 mm during December 29 through December 31, 2019. On December 30th, the average observed
discharge rate at the outlet gage was 4.9 m³/s, peak flow reached to 13.8 m³/s at 20 pm, continued to 14.8 m³/s at 21 pm and
then discharge started to fall. The average simulated discharge was 3.6 m³/s and the peak flow reached 5.4 and 6.9 m³/s at 20
335 and 21 pm respectively.

Generally, the hourly model underestimated the peak flows with values much lower than the observations for the majority of
the events. Observational errors in the model input data may explain the difference between the simulated and observed
values as these errors can generate variability, lead to undesired trends, and influence the model calibration and validation
results. Hydrological models are climate-driven, so of the many types of input data, correct representation of spatial
340 precipitation is essential (Guzman et al., 2015, Kamali et al., 2017).

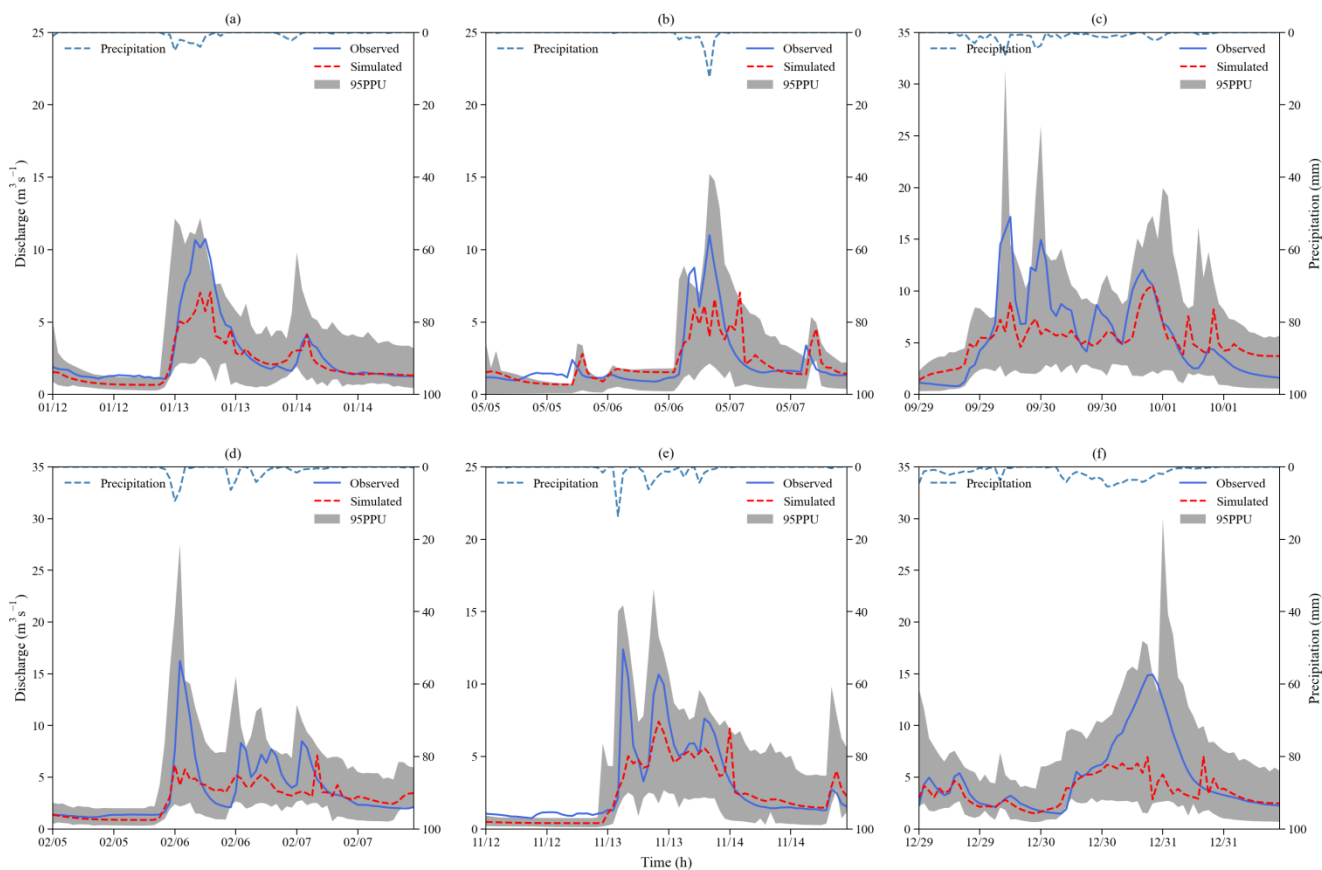


Figure 5. Observed and simulated hourly discharge ($\text{m}^3 \text{s}^{-1}$) for the heavy rainfall events that occurred in 2018 and 2019: (a) event from 12/01-14/01/2018; (b) event from 05/05-07/05/2018; (c) event from 29/09-01/10/2018; (d) event from 05/02-07/02/2019; (e) event from 12/11-14/11/2019; (f) event from 29/12-31/12/2019.

345

4 Conclusions

Experimental catchments provide long term time series of hydrological data which are essential for improved application of best management practices and the development and validation of watershed models. In this study, discharge was monitored for three years (2017-2019) in an experimental basin, located in Athens, Greece. Discharge simulation, calibration and validation were achieved with the application of SWAT model, which has been increasingly used to support decisions on various environmental issues and policy directions. Daily and hourly rainfall observations were used as inputs to SWAT and the model was tested for the period 2017-2019. Surface runoff was estimated using the CN method for the daily model and the GAML method for the hourly model.

350

A sensitivity analysis conducted in this study showed that the parameters related to groundwater flow were more sensitive for daily time intervals and channel routing parameters were more influential for hourly time intervals. These findings

355



indicate that the model operational time step affect parameters' sensitivity to the model output, thus demonstrating the need for different model strategy for the simulation of sub-daily hydrological processes.

360 Generally, the daily model performed better than the sub-daily model in simulating runoff. The CN method produced higher discharge peaks than the GAML method and estimated better the observed values. Quantitative statistics of the observed and the simulated records indicate that the calibration and validation processes produced acceptable results for both infiltration methods. Additionally, graphical techniques at the outlet station show that both models succeed in capturing majority of seasonality and peak discharge. The differences in the calibrated values of the two models lay mostly in the different runoff estimation methods used by the two models.

365 Overall, the general agreement between observations and simulations in both models suggests that the SWAT model appears to be a reliable tool to predict discharge over long periods of time. It should be noted that several factors such as data limitation, observational errors in input data, complexities of spatial and temporal scales and inaccuracies in model structure may lead to uncertainty in model outputs. In the future, emphasis will be placed in the quantification of the parameter uncertainty by including more observed variables in the calibration process such as evapotranspiration and soil moisture satellite data.

370

Code availability. The source codes of the SWAT model are available at the website <http://swat.tamu.edu/> (USDA Agricultural Research Service and Texas A&M AgriLife Research)

375 *Data availability.* The DEM data were downloaded from the website <https://earthexplorer.usgs.gov/> (Shuttle Radar Topography Mission, SRTM). The land use data were downloaded from the website <https://land.copernicus.eu/> (Corine Land Cover, CLC 2018). The soil data were downloaded from the website <http://www.fao.org/> (Food and Agriculture Organization, FAO). The weather data were downloaded from the website <https://www.meteo.gr/> (National Observatory of Athens, NOA). The discharge data were downloaded from the website <https://openhi.net/> (Open Hydrosystem Information Network).

380 *Author contributions.* EK performed the simulations, analyzed the results and prepared the manuscript with contributions from all the co-authors. NM and AK contributed to the conception and methodology of this study. AK was the supervisor of the research project and provided the funding that lead to this publication.

Competing interests. The authors declare that they have no conflict of interest.

385

Acknowledgements. The research work was supported by the Hellenic Foundation for Research and Innovation (HFRI) under the HFRI PhD Fellowship grant (Fellowship Number: 1586). The authors are grateful to Nancy Sammons, Information Technology Specialist of the SWAT team and Chris George, Software Engineer of the SWAT team for their help with the SWAT software.



References

- 390 Abbaspour, K. C., Johnson, C. A. and van Genuchten, M. T.: Estimating Uncertain Flow and Transport Parameters Using a Sequential Uncertainty Fitting Procedure, *Vadose Zo. J.*, 3(4), 1340–1352, doi:10.2113/3.4.1340, 2004.
- Abbaspour, K. C., Yang, J., Maximov, I., Siber, R., Bogner, K., Mieleitner, J., Zobrist, J. and Srinivasan, R.: Modelling hydrology and water quality in the pre-alpine/alpine Thur watershed using SWAT, *J. Hydrol.*, 333(2–4), 413–430, doi:10.1016/j.jhydrol.2006.09.014, 2007.
- 395 Abbaspour, K. C., Rouholahnejad, E., Vaghefi, S., Srinivasan, R., Yang, H. and Kløve, B.: A continental-scale hydrology and water quality model for Europe: Calibration and uncertainty of a high-resolution large-scale SWAT model, *J. Hydrol.*, 524(May), 733–752, doi:10.1016/j.jhydrol.2015.03.027, 2015.
- Arnold, J. G., Srinivasan, R., Mutiah, R. S. and Williams, J. R.: Large Area Hydrologic Modeling and Assessment Part I: Model Development, *J. Am. Water Resour. Assoc.*, 34(1), 73–89, doi:10.1111/j.1752-1688.1998.tb05961.x, 1998.
- 400 Arnold, J. G., Moriasi, D. N., Gassman, P. W., Abbaspour, K. C., White, M. J., Srinivasan, R., Santhi, C., Harmel, R. D., Van Griensven, A., Van Liew, M. W., Kannan, N. and Jha, M. K.: SWAT: Model Use, Calibration, and Validation, *Trans. ASABE*, 55(4coper), 1491–1508, doi:10.13031/2013.42256, 2012.
- Arnold, J. G., Youssef, M. A., Yen, H., White, M. J., Sheshukov, A. Y., Sadeghi, A. M., Moriasi, D. N., Steiner, J. L., Amatya, D. M., Skaggs, R. W., Haney, E. B., Jeong, J., Arabi, M. and Gowda, P. H.: Hydrological Processes and Model
- 405 Representation: Impact of Soft Data on Calibration, *Trans. ASABE*, 58(6), 1637–1660, doi:10.13031/trans.58.10726, 2015.
- Bauwe, A., Kahle, P. and Lennartz, B.: Hydrologic evaluation of the curve number and Green and Ampt infiltration methods by applying Hooghoudt and Kirkham tile drain equations using SWAT, *J. Hydrol.*, 537, 311–321, doi:10.1016/j.jhydrol.2016.03.054, 2016.
- Bauwe, A., Tiedemann, S., Kahle, P. and Lennartz, B.: Does the Temporal Resolution of Precipitation Input Influence the
- 410 Simulated Hydrological Components Employing the SWAT Model?, *J. Am. Water Resour. Assoc.*, 53(5), 997–1007, doi:10.1111/1752-1688.12560, 2017.
- Bogena, H. R., White, T., Bour, O., Li, X. and Jensen, K. H.: Toward Better Understanding of Terrestrial Processes through Long-Term Hydrological Observatories, *Vadose Zo. J.*, 17(1), 180194, doi:10.2136/vzj2018.10.0194, 2018.
- Boithias, L., Sauvage, S., Lenica, A., Roux, H., Abbaspour, K., Larnier, K., Dartus, D. and Sánchez-Pérez, J.: Simulating
- 415 Flash Floods at Hourly Time-Step Using the SWAT Model, *Water*, 9(12), 929, doi:10.3390/w9120929, 2017.
- Brightenti, T. M., Bonumá, N. B., Srinivasan, R. and Chaffe, P. L. B.: Simulating sub-daily hydrological process with SWAT: a review, *Hydrol. Sci. J.*, 64(12), 1415–1423, doi:10.1080/02626667.2019.1642477, 2019.
- Campbell, A., Pradhanang, S. M., Kouhi Anbaran, S., Sargent, J., Palmer, Z. and Audette, M.: Assessing the impact of urbanization on flood risk and severity for the Pawtuxet watershed, Rhode Island, *Lake Reserv. Manag.*, 34(1), 74–87,
- 420 doi:10.1080/10402381.2017.1390016, 2018.
- Cheng, Q. B., Reinhardt-Imjela, C., Chen, X., Schulte, A., Ji, X. and Li, F. L.: Improvement and comparison of the rainfall–



- runoff methods in SWAT at the monsoonal watershed of Baocun, Eastern China, *Hydrol. Sci. J.*, 61(8), 1460–1476, doi:10.1080/02626667.2015.1051485, 2016.
- Corine Land Cover, (CLC): Land use data, [online] Available from: <https://land.copernicus.eu/> (Accessed 15 December 425 2020), 2018.
- Daggupati, P., Yen, H., White, M. J., Srinivasan, R., Arnold, J. G., Keitzer, C. S. and Sowa, S. P.: Impact of model development, calibration and validation decisions on hydrological simulations in West Lake Erie Basin, *Hydrol. Process.*, 29(26), 5307–5320, doi:10.1002/hyp.10536, 2015a.
- Daggupati, P., Yen, H., White, M. J., Srinivasan, R., Arnold, J. G., Keitzer, C. S. and Sowa, S. P.: Impact of model 430 development, calibration and validation decisions on hydrological simulations in West Lake Erie Basin, *Hydrol. Process.*, 29(26), 5307–5320, doi:10.1002/hyp.10536, 2015b.
- Dile, Y. T., Daggupati, P., George, C., Srinivasan, R. and Arnold, J.: Introducing a new open source GIS user interface for the SWAT model, *Environ. Model. Softw.*, 85, 129–138, doi:10.1016/j.envsoft.2016.08.004, 2016.
- Douglas-Mankin, K. R., Srinivasan, R. and Arnold, J. G.: Soil and Water Assessment Tool (SWAT) Model: Current 435 Developments and Applications, *Trans. ASABE*, 53(5), 1423–1431, doi:10.13031/2013.34915, 2010.
- Engel, B., Storm, D., White, M., Arnold, J. and Arabi, M.: A Hydrologic/Water Quality Model Application, *J. Am. Water Resour. Assoc.*, 43(5), 1223–1236, doi:10.1111/j.1752-1688.2007.00105.x, 2007.
- FAO, IIASA, ISRIC and ISSCAS: Harmonized World Soil Database Version 1.2, Food & Agriculture Organization of the UN, Rome, Italy, and International Institute for Applied Systems Analysis, Laxenburg, Austria., 2012.
- Ficklin, D. L. and Zhang, M.: A Comparison of the Curve Number and Green-Ampt Models in an Agricultural Watershed, 440 *Trans. ASABE*, 56(1), 61–69, doi:10.13031/2013.42590, 2013.
- Food and Agriculture Organization, (FAO): HWSD soil data, [online] Available from: www.fao.org (Accessed 10 December 2020), 2012.
- Gassman, P. W., Reyes, M. R., Green, C. H. and Arnold, J. G.: The Soil and Water Assessment Tool: Historical 445 Development, Applications, and Future Research Directions, *Trans. ASABE*, 50(4), 1211–1250, doi:10.13031/2013.23637, 2007.
- Gassman, P. W., Sadeghi, A. M. and Srinivasan, R.: Applications of the SWAT Model Special Section: Overview and Insights, *J. Environ. Qual.*, 43(1), 1–8, doi:10.2134/jeq2013.11.0466, 2014.
- Golmohammadi, G., Rudra, R., Dickinson, T., Goel, P. and Veliz, M.: Predicting the temporal variation of flow contributing 450 areas using SWAT, *J. Hydrol.*, 547, 375–386, doi:10.1016/j.jhydrol.2017.02.008, 2017.
- Goodrich, D. C., Heilman, P., Anderson, M., Baffaut, C., Bonta, J., Bosch, D., Bryant, R., Cosh, M., Endale, D., Veith, T. L., Havens, S. C., Hedrick, A., Kleinman, P. J., Langendoen, E. J., McCarty, G., Moorman, T., Marks, D., Pierson, F., Rigby, J. R., Schomberg, H., Starks, P., Steiner, J., Strickland, T. and Tsegaye, T.: The USDA-ARS Experimental Watershed Network: Evolution, Lessons Learned, Societal Benefits, and Moving Forward, *Water Resour. Res.*, 57(2), 0–3, 455 doi:10.1029/2019WR026473, 2020.



- Gupta, H. V., Sorooshian, S. and Yapo, P. O.: Status of Automatic Calibration for Hydrologic Models: Comparison with Multilevel Expert Calibration, *J. Hydrol. Eng.*, 4(2), 135–143, doi:10.1061/(asce)1084-0699(1999)4:2(135), 1999.
- Guzman, J. A., Shirmohammadi, A., Sadeghi, A. M., Wang, X., Chu, M. L., Jha, M. K., Parajuli, P. B., Harmel, R. D., Khare, Y. P. and Hernandez, J. E.: Uncertainty considerations in calibration and validation of hydrologic and water quality
460 models, *Trans. ASABE*, 58(6), 1745–1762, doi:10.13031/trans.58.10710, 2015.
- Han, E., Merwade, V. and Heathman, G. C.: Implementation of surface soil moisture data assimilation with watershed scale distributed hydrological model, *J. Hydrol.*, 416–417, 98–117, doi:10.1016/j.jhydrol.2011.11.039, 2012.
- Harmel, R. D., Smith, P. K., Migliaccio, K. W., Chaubey, I., Douglas-Mankin, K. R., Benham, B., Shukla, S., Muñoz-Carpena, R. and Robson, B. J.: Evaluating, interpreting, and communicating performance of hydrologic/water quality models
465 considering intended use : A review and recommendations, *Environ. Model. Softw.*, 21, 40–51, 2014.
- Hrachowitz, M., Benettin, P., van Breukelen, B. M., Fovet, O., Howden, N. J. K., Ruiz, L., van der Velde, Y. and Wade, A. J.: Transit times-the link between hydrology and water quality at the catchment scale, *Wiley Interdiscip. Rev. Water*, 3(5), 629–657, doi:10.1002/wat2.1155, 2016.
- Hubbart, J. A., Kellner, E. and Zeiger, S. J.: A Case-Study Application of the Experimental Watershed Study Design to
470 Advance Adaptive Management of Contemporary Watersheds, *Water*, 11(11), 2355, doi:10.3390/w11112355, 2019.
- Jeong, J., Kannan, N., Arnold, J., Glick, R., Gosselink, L. and Srinivasan, R.: Development and Integration of Sub-hourly Rainfall-Runoff Modeling Capability Within a Watershed Model, *Water Resour. Manag.*, 24(15), 4505–4527, doi:10.1007/s11269-010-9670-4, 2010.
- Kamali, B., Abbaspour, K. C. and Yang, H.: Assessing the uncertainty of multiple input datasets in the prediction of water
475 resource components, *Water (Switzerland)*, 9(9), doi:10.3390/w9090709, 2017.
- Kannan, N., White, S. M., Worrall, F. and Whelan, M. J.: Sensitivity analysis and identification of the best evapotranspiration and runoff options for hydrological modelling in SWAT-2000, *J. Hydrol.*, 332(3–4), 456–466, doi:10.1016/j.jhydrol.2006.08.001, 2007.
- Kellner, E. and Hubbart, J. A.: Application of the experimental watershed approach to advance urban watershed
480 precipitation/discharge understanding, *Urban Ecosyst.*, 20(4), 799–810, doi:10.1007/s11252-016-0631-4, 2017.
- King, K. W., Arnold, J. G. and Bingner, R. L.: Comparison of Green-Ampt and curve number methods on Goodwin Creek Watershed using SWAT, *Trans. Am. Soc. Agric. Eng.*, 42(4), 919–925, doi:10.13031/2013.13272, 1999.
- Kouchi, D. H., Esmaili, K., Faridhosseini, A., Sanaeinejad, S. H., Khalili, D. and Abbaspour, K. C.: Sensitivity of calibrated parameters and water resource estimates on different objective functions and optimization algorithms, *Water (Switzerland)*,
485 9(6), 1–16, doi:10.3390/w9060384, 2017.
- Li, X., Cheng, G., Liu, S., Xiao, Q., Ma, M., Jin, R., Che, T., Liu, Q., Wang, W., Qi, Y., Wen, J., Li, H., Zhu, G., Guo, J., Ran, Y., Wang, S., Zhu, Z., Zhou, J., Hu, X. and Xu, Z.: Heihe Watershed Allied Telemetry Experimental Research (HiWATER): Scientific Objectives and Experimental Design, *Bull. Am. Meteorol. Soc.*, 94(8), 1145–1160, doi:10.1175/BAMS-D-12-00154.1, 2013.



- 490 Li, Y. and DeLiberty, T.: Evaluating hourly SWAT streamflow simulations for urbanized and forest watersheds across northwestern Delaware, US, *Stoch. Environ. Res. Risk Assess.*, 0123456789, doi:10.1007/s00477-020-01904-y, 2020.
- Maharjan, G. R., Park, Y. S., Kim, N. W., Shin, D. S., Choi, J. W., Hyun, G. W., Jeon, J. H., Ok, Y. S. and Lim, K. J.: Evaluation of SWAT sub-daily runoff estimation at small agricultural watershed in Korea, *Front. Environ. Sci. Eng. China*, 7(1), 109–119, doi:10.1007/s11783-012-0418-7, 2013.
- 495 Mein, R.G. and Larson, C. L.: Modeling Infiltration during a Steady Rain, *Water Resour. Res.*, 9(2), 384–394, 1973.
- Moriasi, D. N., Arnold, J. G., Van Liew, M. W., Bingner, R. L., Harmel, R. D. and Veith, T. L.: Model Evaluation Guidelines for Systematic Quantification of Accuracy in Watershed Simulations, *Trans. ASABE*, 50(3), 885–900, doi:10.13031/2013.23153, 2007.
- Moriasi, D. N., Gitau, M. W., Pai, N. and Daggupati, P.: Hydrologic and water quality models: Performance measures and evaluation criteria, *Trans. ASABE*, 58(6), 1763–1785, doi:10.13031/trans.58.10715, 2015.
- 500 Nash, J. E. and Sutcliffe, J. V.: River flow forecasting through conceptual models part I - A discussion of principles, *J. Hydrol.*, 10(3), 282–290, doi:10.1016/0022-1694(70)90255-6, 1970.
- National Observatory of Athens, (NOA): Weather data, [online] Available from: <https://www.meteo.gr/> (Accessed 10 December 2020).
- 505 Neitsch, S. L., Arnold, J. G., Kiniry, J. R. and Williams, J. R.: Soil & Water Assessment Tool Theoretical Documentation Version 2009, Texas Water Resources Institute Technical Report No. 406, Texas, USA., 2011.
- Nichols, J., Hubbart, J. A. and Poulton, B. C.: Using macroinvertebrate assemblages and multiple stressors to infer urban stream system condition: a case study in the central US, *Urban Ecosyst.*, 19(2), 679–704, doi:10.1007/s11252-016-0534-4, 2016.
- 510 Open Hydrosystem Information Network, (OpenHi.net): Observed streamflow data, [online] Available from: <https://openhi.net/> (Accessed 20 December 2020).
- Polanco, E. I., Fleifle, A., Ludwig, R. and Disse, M.: Improving SWAT model performance in the upper Blue Nile Basin using meteorological data integration and subcatchment discretization, *Hydrol. Earth Syst. Sci.*, 21(9), 4907–4926, doi:10.5194/hess-21-4907-2017, 2017.
- 515 Smart Toolbox for Engaging Citizens in a People-Centric Observation Web, (SCENT): Discharge stations, [online] Available from: <https://scent-project.eu/> (Accessed 20 December 2020).
- Soil Conservation Service, S.: National Engineering Handbook, Section 4, Hydrology, Department of Agriculture, Washington DC, USA., 1972.
- Stockinger, M. P., Bogena, H. R., Lücke, A., Diekkrüger, B., Cornelissen, T. and Vereecken, H.: Tracer sampling frequency influences estimates of young water fraction and streamwater transit time distribution, *J. Hydrol.*, 541, 952–964, doi:10.1016/j.jhydrol.2016.08.007, 2016.
- 520 Tan, M. L., Gassman, P. W., Yang, X. and Haywood, J.: A review of SWAT applications, performance and future needs for simulation of hydro-climatic extremes, *Adv. Water Resour.*, 143(June), 103662, doi:10.1016/j.advwatres.2020.103662,



- 2020.
- 525 Tauro, F., Selker, J., van de Giesen, N., Abrate, T., Uijlenhoet, R., Porfiri, M., Manfreda, S., Caylor, K., Moramarco, T., Benveniste, J., Ciraolo, G., Estes, L., Domeneghetti, A., Perks, M. T., Corbari, C., Rabiei, E., Ravazzani, G., Bogena, H., Harfouche, A., Brocca, L., Maltese, A., Wickert, A., Tarpanelli, A., Good, S., Lopez Alcala, J. M., Petroselli, A., Cudennec, C., Blume, T., Hut, R. and Grimaldi, S.: Measurements and Observations in the XXI century (MOXXI): innovation and multi-disciplinarity to sense the hydrological cycle, *Hydrol. Sci. J.*, 63(2), 169–196, doi:10.1080/02626667.2017.1420191,
- 530 2018.
- U.S. Geological Survey, (USGS): Shuttle Radar Topography Mission (SRTM), DEM data, [online] Available from: <https://earthexplorer.usgs.gov/> (Accessed 5 December 2020).
- White, T., Brantley, S., Banwart, S., Chorover, J., Dietrich, W., Derry, L., Lohse, K., Anderson, S., Aufdendkampe, A., Bales, R., Kumar, P., Richter, D. and McDowell, B.: The Role of Critical Zone Observatories in Critical Zone Science, in
- 535 *Developments in Earth Surface Processes*, vol. 19, pp. 15–78, Elsevier B.V., 2015.
- Yang, X., Liu, Q., He, Y., Luo, X. and Zhang, X.: Comparison of daily and sub-daily SWAT models for daily streamflow simulation in the Upper Huai River Basin of China, *Stoch. Environ. Res. Risk Assess.*, 30(3), 959–972, doi:10.1007/s00477-015-1099-0, 2016.
- Yu, D., Xie, P., Dong, X., Hu, X., Liu, J., Li, Y., Peng, T., Ma, H., Wang, K. and Xu, S.: Improvement of the SWAT model
- 540 for event-based flood simulation on a sub-daily timescale, *Hydrol. Earth Syst. Sci.*, 22(9), 5001–5019, doi:10.5194/hess-22-5001-2018, 2018.
- Zacharias, S., Bogena, H., Samaniego, L., Mauder, M., Fuß, R., Pütz, T., Frenzel, M., Schwank, M., Baessler, C., Butterbach-Bahl, K., Bens, O., Borg, E., Brauer, A., Dietrich, P., Hajnsek, I., Helle, G., Kiese, R., Kunstmann, H., Klotz, S., Munch, J. C., Papen, H., Priesack, E., Schmid, H. P., Steinbrecher, R., Rosenbaum, U., Teutsch, G. and Vereecken, H.: A
- 545 Network of Terrestrial Environmental Observatories in Germany, *Vadose Zo. J.*, 10(3), 955–973, doi:10.2136/vzj2010.0139, 2011.
- Zeiger, S. J. and Hubbart, J. A.: Nested-Scale Nutrient Flux in a Mixed-Land-Use Urbanizing Watershed, *Hydrol. Process.*, 30(10), 1475–1490, doi:10.1002/hyp.10716, 2016.